Development of the CBM RICH readout electronics and DAQ.

Prototype results, time resolution with and without WLS coverage, WLS fluorescence.

E. Ovcharenko[1,2], S. Belogurov[3,1] and M. Dürr[4] for the CBM-RICH collaboration

eovchar@jinr.ru
1 – LIT JINR, Dubna, Russia
2 – ITEP, Moscow, Russia
3 – NRNU MEPhI
4 – Justus-Liebig Universität Giessen, Germany

Supported by FRRC, Hic4Fair and BMBF.

Introduction

The CBM experiment at the future FAIR facility (Darmstadt, Germany) will investigate strongly interacting matter at high net-baryon densities but moderate temperatures in heavy-ion collisions. The CBM RICH detector is required for identifying di-electrons in a momentum range up to 8 GeV/c. It is a classical RICH detector with gaseous radiator, spherical mirrors and segmented photosensitive camera made of ~1000 Hamamatsu H12700 multi-anode photomultiplier tubes. The MAPMTs will be read out by self-triggered FPGA-based frond end boards detecting only time information.

CBM RICH Tech. Design Report:

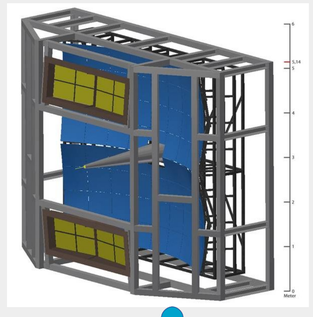

Common CBM beam tests at PS, CERN, Nov 2014

During our Nov 2014 CERN-PS beamtime a CBM RICH prototype including a camera of 16 MAPMTs partially covered with p-terphenyl as WLS coating has been succefully tested. The MAPMTs were read out by 64 PADIWAs and 64 TDCs on 16 TRBs. Readout via two parallel chains has been performed – using FLES Interface Board (FLIB) and using standard Ethernet via router to Network Interface Card (NIC).

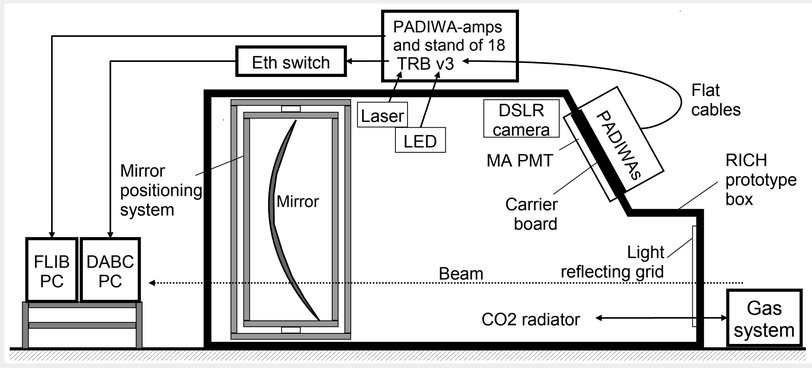

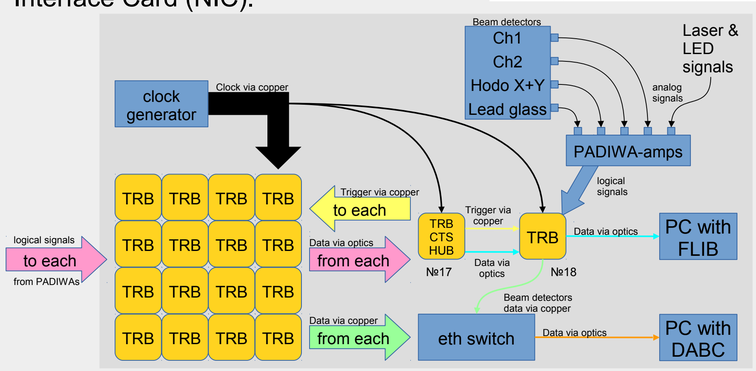

TRB – TRB with "standard" firmware – 4 TDCs and hub; 4 addon boards – adaptors for flat cables transmitting LVDS from PADIWAs

TRB CTS HUB – TRB with "CTS+4HUBs" firmware; 4 addon boards, each 8 input optical links; trigger distributed using one RG45 output of TRB into LVDS fanout boards

J. Adamczewski-Musch et al., Influence of wavelength-shifting films on multianode PMTs with UV-extended windows. Nucl.Instr.Meth. A 783 (2015) 43.

CBM RICH readout chain prototype

TRB

http://trb.gsi.de/

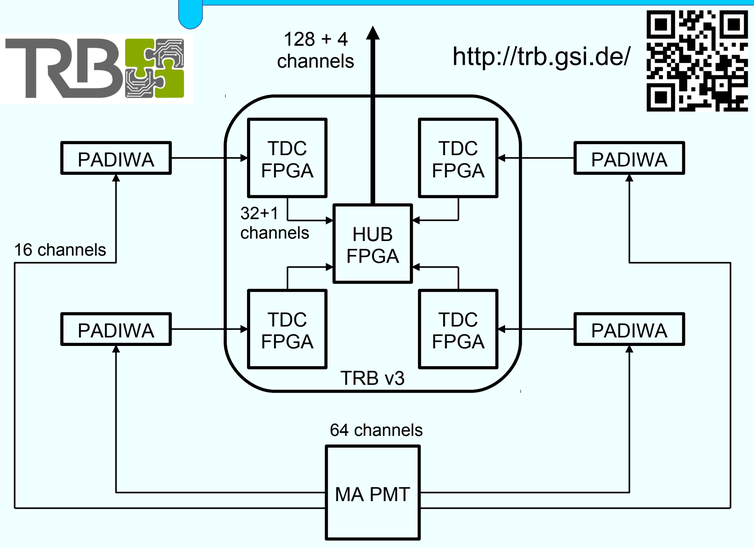

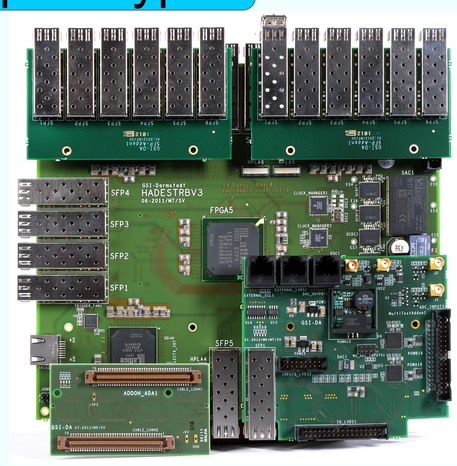

M. Traxler e al, JINST 6 12004 (2011)
A. Neiser e al, JINST 8 (2013) C12043

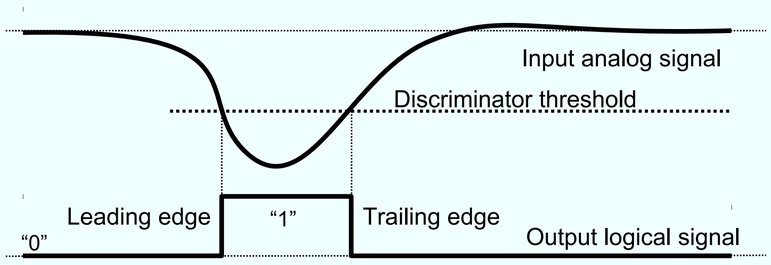

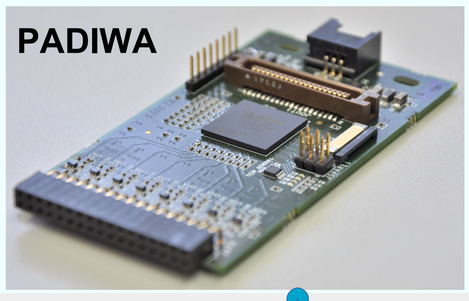

Fine time calibration stability over one run

The stability of the fine time calibration has been studied using the laboratory measurements.
A typical calibration table with linear function subtracted is shown below.

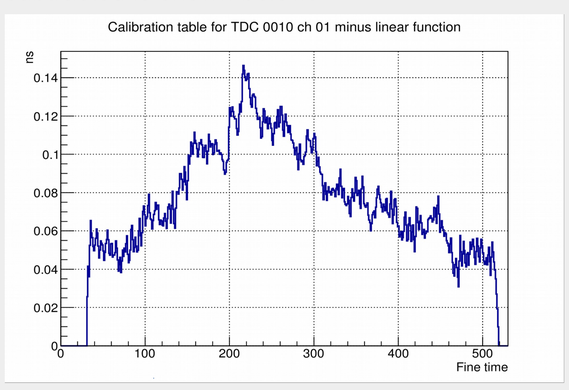

Calibration table of some subsets of data minus calibration table built from the full run: Blue – first 15%; Red – last 15%; Green – middle 15%. All within 22 ps.

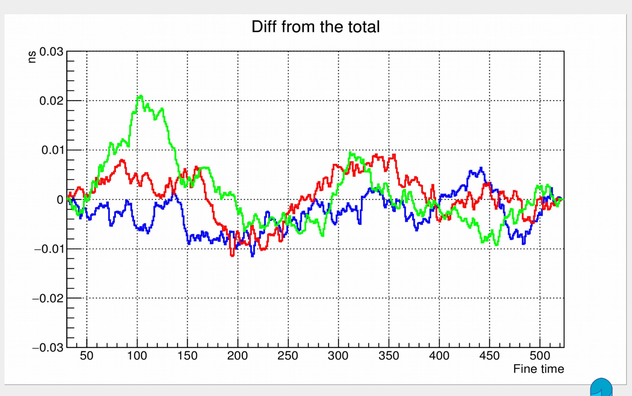

Single electron spectrum from the threshold scan

The measurements with different discriminator thresholds have been performed in the laboratory. The counter of the detected timestamps in a TDC channel has been used to obtain the dependency of the hit rate from the threshold. This threshold scan dependency was then fitted with an analytical 7-th order polynomial function (red line). The bottom figure shows the analytical derivative of the approximating curve. It corresponds to a single electron spectrum which can not be directly obtained using a readout chain without amplitude detection.

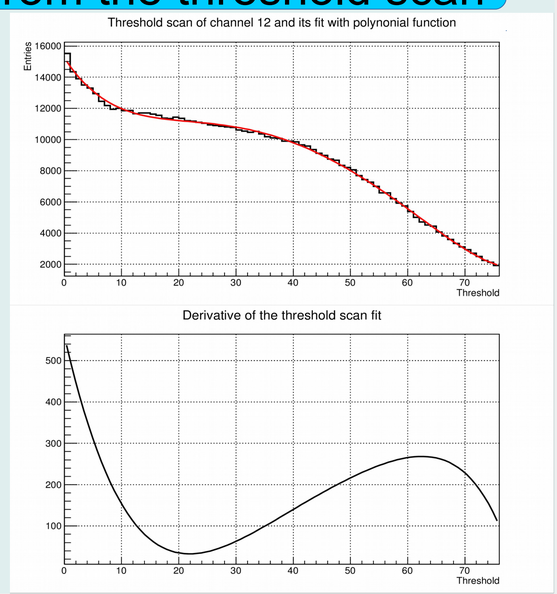

Direct TDC measurements. TDC time precision and calibration effect.

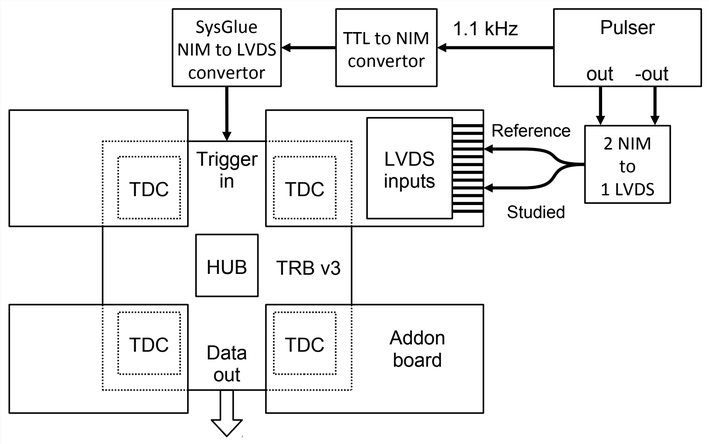

A 10ns-wide pulse from a high-precision pulser was split into two and sent directly to different pairs of the TDC input channels using identical cables. An example of the distribution of the difference between the two registered timestamps and the registered pulse width are shown in the bottom figures before and after fine time calibration.
All distributions are shown without inter-channel corrections.
All RMS less than 20 ps.

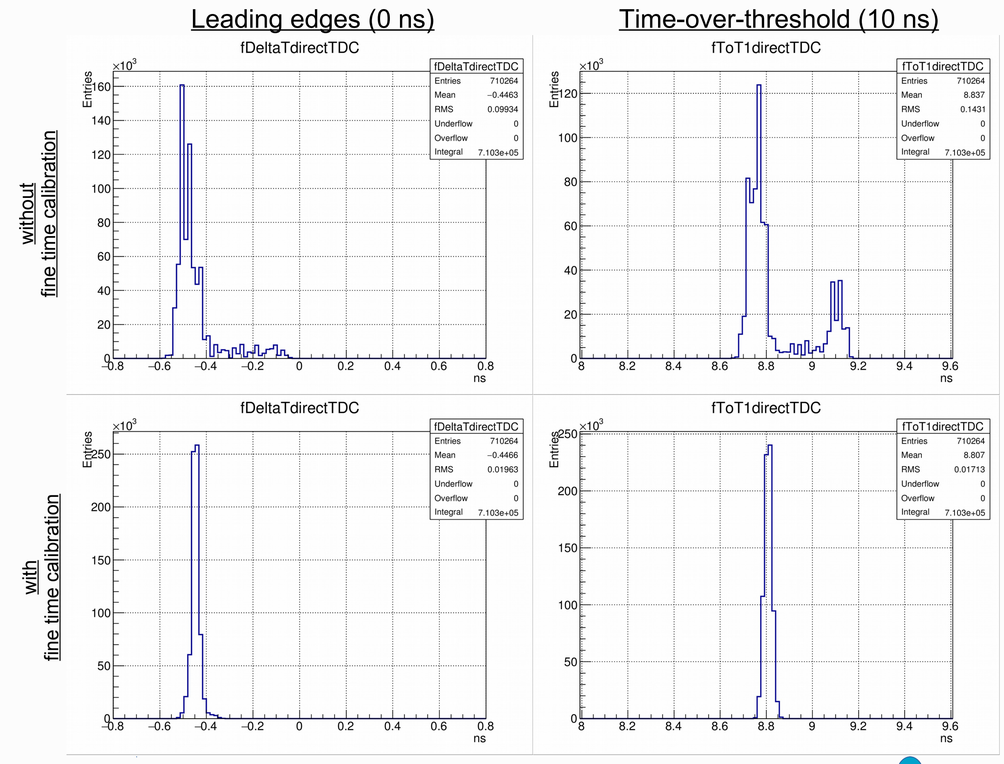

Full readout chain time precision

The time precision of the full readout chain has been obtained from the beamtime data.
"Leading edge difference" distributions for 4 areas of the camera:

- Blue – 2 certain channels.
- Red – 16 channels of 1 PADIWA.
- Green – 64 channels of 1 PMT.
- Black – 256 channels of 4 PMTs (2 by 2 PMTs top-right quarter of the camera).

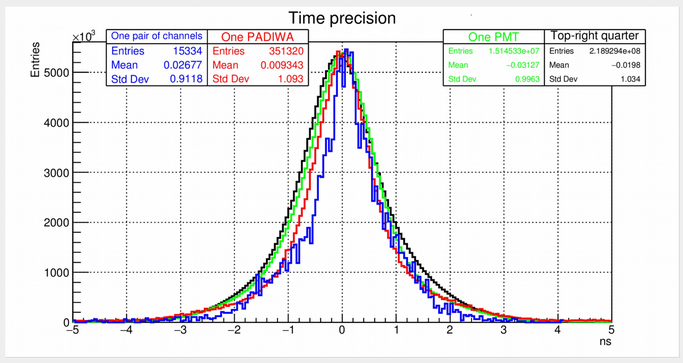

The distributions are scaled for visual comparison.

p-terphenyl WLS effect on timing

During RICH prototype beam tests there were 3 groups of PMTs in the camera: (1) covered with WLS layers for the first runs, then cleaned and used without WLS films for the second set of runs, (2) covered with WLS layers for the whole beamtime and (3) not covered for the whole beamtime. By comparison of the data received using the PMTs from the first group (1) we can analyse the effect of WLS layers.
Beam events may contain Cherenkov rings on the camera plane. The analysis technique for the time precision is based on the fact that signals in different channels within one event coming from one laser flash or one charged particle emitting Cherenkov light are simultaneous.
In each event, the first hit in time is used to define the reference time tref. For all other hits in the event, the time difference, $\Delta t_i = t_i - t_{ref}$, $i \neq ref$ is computed. The Δt distributions for two sets of data are shown in the top figure.
Subtracting the blue distribution (no WLS layer) from the red (WLS layer), we subtract the timing information for all hits not being affected by the WLS layer. The resulting WLS time profile is shown in the bottom figure. It consists of two major exponential components with decay times τ_1 and τ_2,

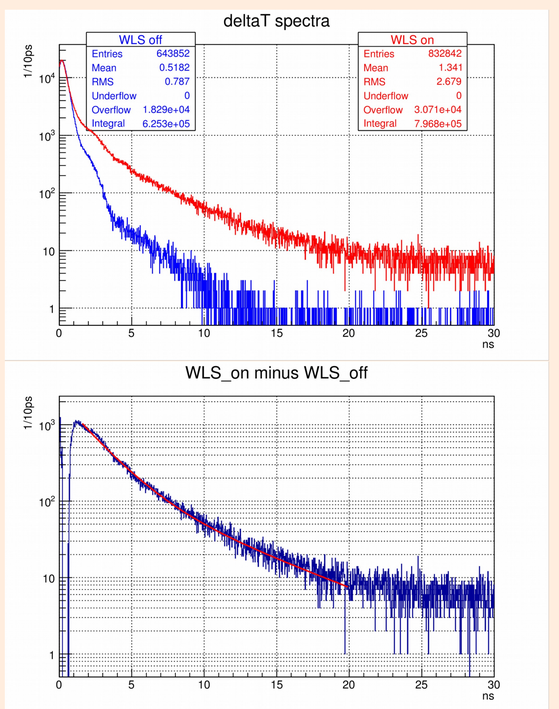

so the difference is fitted by $f(t) = A \cdot e^{-t/\tau_1} + B \cdot e^{-t/\tau_2} \qquad t \in [1.5\,ns, 20\,ns]$

Thus the measured p-terphenyl WLS time profile consists of two components:
τ_1=1.92ns and ***τ_2=5.69ns.***

WLS fluorescence measurement

- Time-dependent fluorescence of WLS films similar to the films used on MAPMTs.
- Excitation at 280 nm, emission at 380 nm.
- The experimental data can be fitted using three time constants:
  τ_1 = 1.4 ns, τ_2 = 3.8 ns, and **τ_3 = 45 ns.**